

Mediation of c-Myc–Induced Apoptosis by p53

Heiko Hermeking and Dirk Eick*

The cellular proto-oncogene *c-myc* is involved in cell proliferation and transformation but is also implicated in the induction of programmed cell death (apoptosis). The same characteristics have been described for the tumor suppressor gene *p53*, the most commonly mutated gene in human cancer. In quiescent mouse fibroblasts expressing wild-type p53 protein, activation of c-Myc was found to induce apoptosis and cell cycle reentry, preceded by stabilization of p53. In contrast, in quiescent p53-null fibroblasts, activation of c-Myc induced cell cycle reentry but not apoptosis. These results suggest that p53 mediates apoptosis as a safeguard mechanism to prevent cell proliferation induced by oncogene activation.

The cellular proto-oncogene *c-myc* and the tumor suppressor gene *p53* encode ubiquitously expressed nuclear phosphoproteins that function as transcriptional regulators controlling cell proliferation, differentiation, and apoptosis (1, 2). The c-Myc protein is a positive regulator of cell cycle progression and is sufficient for induction of cell cycle reentry, whereas the wild-type p53 protein is a negative regulator that arrests cells in G₁. Both proteins have short half-lives and modulate the expression of target genes by binding to specific DNA sequences (3, 4). Here, we have studied the functional interaction of c-Myc and p53 in the induction of apoptosis.

Serum-starved mouse and rat fibroblasts that express a chimeric protein consisting of the full-length c-Myc protein fused to the hormone-binding domain of the human estrogen receptor (c-MycER) show c-Myc activity only in the presence of β-estradiol (4). With β-estradiol, the cells reenter the cell cycle and undergo apoptosis, whereas in the absence of β-estradiol the cells arrest in a G₀-like state (2, 4). Five NIH 3T3-L1 mouse fibroblast cell lines (LM-3, LM-4, LM-6, LM-7, and LM-8) stably expressing c-MycER were established (5). Sequence analysis confirmed that LM-3 and parental NIH 3T3-L1 cells express wild-type p53 (6). Activation of c-MycER by the addition of β-estradiol induced DNA synthesis and cell death in serum-starved LM-3 cells (Fig. 1) (5). Cell death showed characteristic features of apoptosis, including chromatin condensation, nuclear fragmentation, and cytoplasmic blebbing (Fig. 1, A and B). Twenty-four hours after activation of c-Myc, ~40% of the cells in the five LM cell lines had died (Fig. 1E). Of the remaining viable cells, 40 to 80% had entered the S phase, as visualized by incorporation of 5-bromo-2'-deoxyuridine (BrdU) (Fig. 1, C

and F). Similar results were obtained with NIH 3T3 mouse fibroblasts expressing c-MycER from a retroviral long terminal repeat (LTR) promoter (Fig. 1, E and F).

Activation of c-Myc led to an accumulation of p53 protein in quiescent LM-3 cells (Fig. 1D). The p53 protein also accumulated in the four other LM cell clones, in NIH 3T3. LTR-MycER cells, and after addition of hydroxy-tamoxifen, but not when parental NIH 3T3-L1 cells were treated with β-estradiol or hydroxy-tamoxifen (6). The increase in amounts of p53 in LM-3

cells was detectable as early as 1 hour after addition of β-estradiol. By 24 hours, amounts of p53 had increased more than 10-fold (Fig. 2A) (7), whereas amounts of p53 mRNA had increased only 2- to 3-fold (Fig. 2B) (8).

Because the increase in RNA levels could not account for the accumulation of p53 protein, we investigated the effect of c-Myc activation on the stability of the p53 protein. When LM-3 cells were treated with β-estradiol for 16 hours and then with the protein synthesis inhibitor cycloheximide for 2 hours, there was no reduction in amounts of p53 (6). Because wild-type p53 has a half-life of 6 to 20 min (9), this result suggests that p53 is stabilized by c-Myc activation. The stabilized p53 was not reactive with the antibody PAb 240 (6), which is specific for the protein's mutant conformation, but did react with the antibody PAb 122, which recognizes both the mutant and the wild-type conformations (Fig. 1D).

Stabilization of the p53 protein has been shown to prevent entry into the S phase by arresting cells in the G₁ phase (10). In LM-3 cells, c-Myc activation overrides a p53-mediated G₁ arrest because cells that stained positive for p53 were also positive for DNA synthesis (Fig. 1, C and D). This

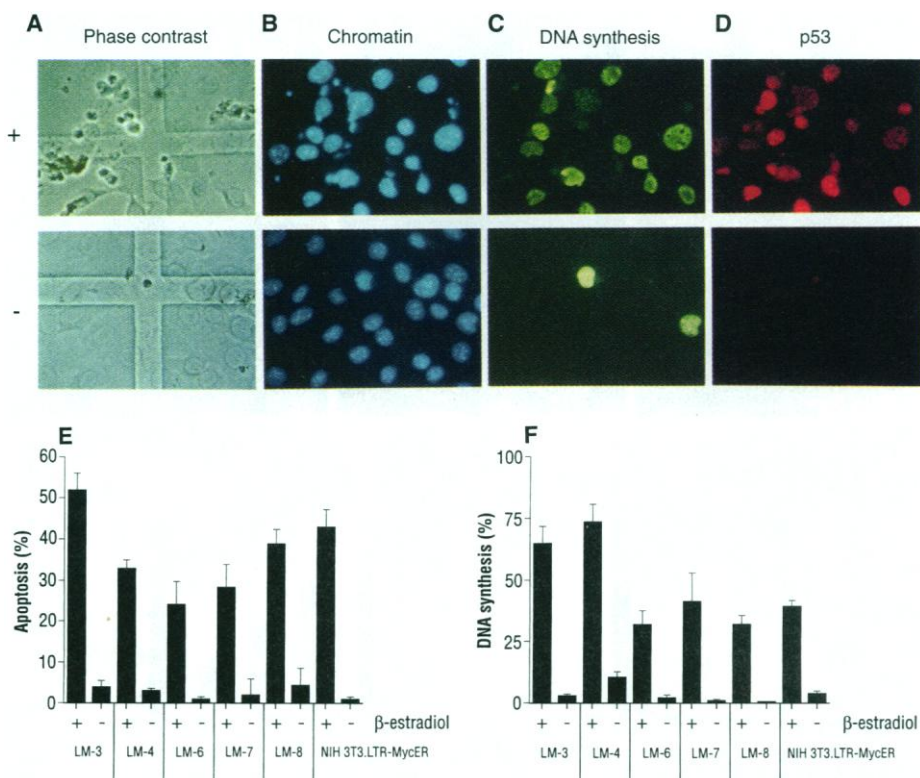


Fig. 1. Induction of p53 protein by activation of c-Myc in serum-starved LM-3 cells. Cells were cultured in the presence (+) or absence (-) of β-estradiol for 24 hours. DNA synthesis was monitored by incorporation of BrdU. Cells are shown (A) in phase-contrast view or after staining with (B) bisbenzamide H 33258, (C) fluorescein-coupled mouse antibody to BrdU, or (D) the PAb 122 antibody to p53 (magnification, ×400). (E and F) Quantification of (E) cells eliminated by apoptosis in the indicated serum-starved cell clones and (F) DNA synthesis 24 hours after addition of β-estradiol. Error bars refer to standard error.

Institut für Klinische Molekularbiologie und Tumorgenetik, Forschungszentrum für Umwelt und Gesundheit, GSF, Marchioninistrasse 25, D-81377 München, Germany.

*To whom correspondence should be addressed.

observation indicates that abrogation of wild-type p53-induced G₁ arrest by c-Myc may be a trigger for apoptosis.

We have recently shown that simian virus 40 large T antigen can antagonize c-Myc-induced apoptosis in NIH 3T3-L1

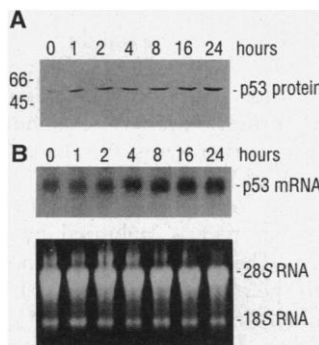


Fig. 2. Levels of p53 protein and mRNA after activation of c-Myc in serum-starved LM-3 cells. **(A)** Immunoblot analysis of p53 protein with PAB 240. Molecular size markers are on the left in kilodaltons. **(B)** Northern blot analysis of p53 mRNA. Shown below the blot is the ethidium bromide-stained RNA before transfer.

cells and that this effect is associated with the binding of p53 to large T antigen (11). To determine if p53 is required for c-Myc-induced apoptosis, we expressed the conditional c-MycER in p53^{-/-} cells. Mouse embryo fibroblasts (MEFs) derived from p53-null mice (12) were stably transfected with the c-MycER construct (5). Second passage p53^{-/-} MEFs were used to rule out the possibility that differences in the apoptotic behavior were due to genetic alterations selected for by cell culture conditions. The initial experiments were carried out with polyclonal pools of transfectants that contained >50% c-MycER-positive cells. After serum starvation of the transfectants for 48 hours, activation of c-Myc by addition of β -estradiol induced DNA synthesis in 20 to 30% of the cells without any indication of apoptosis above background levels (6). Induction of DNA synthesis by addition of β -estradiol was not observed in serum-starved parental p53^{-/-} MEFs. Four p53^{-/-} MEF cell lines expressing c-MycER (NPM-1, NPM-2, NPM-3, and NPM-4) were studied in a similar way. After activation of c-Myc,

increased levels of apoptosis, whereas cells of all four lines entered the S phase (Fig. 3).

These results show that induction of p53 is part of the cellular response to activation of c-Myc in quiescent cells. Whereas serum stimulation of cells is accompanied by a moderate induction of p53 not attributable to protein stabilization (9), activation of c-Myc in the absence of other growth signals leads to the accumulation of stabilized p53 protein. The mechanism of p53 stabilization is unknown. In mouse fibroblasts, c-Myc is dominant over p53-mediated growth arrest and can drive cells from the G₁ into the S phase despite large amounts of wild-type p53 protein. In this situation, p53 may induce cell death by triggering the apoptotic machinery. The absence of c-Myc-induced apoptosis in p53^{-/-} cells demonstrates that c-Myc-induced apoptosis is mediated by p53. Previous work has shown that wild-type p53 also mediates apoptosis induced by the adenoviral oncoprotein E1A (13). Thus, p53-induced apoptosis may be a common tumor suppressive mechanism to eliminate cells that, through expression of oncogenes, inappropriately bypass the G₁-S checkpoint. Deregulated expression of c-Myc and loss of wild-type p53 function are found in many types of tumors. Our results indicate that these two events cooperate in tumor development.

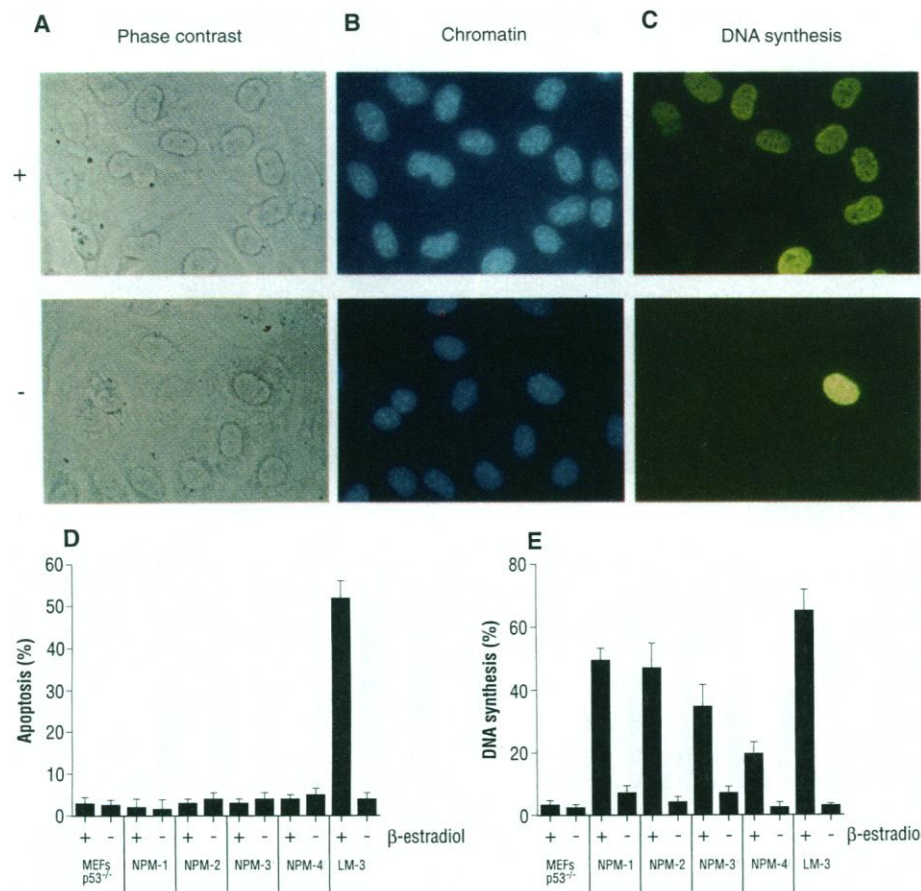


Fig. 3. Effect of c-Myc on serum-starved p53^{-/-} MEFs. The p53^{-/-} MEFs were transfected with HH275.3 DNA, and hygromycin B-resistant bulk cultures or single-cell clones (NPM-1, NPM-2, NPM-3, and NPM-4) were selected and analyzed. **(A to C)** NPM-1 cells were serum-starved, treated with β -estradiol, and analyzed as described (5). **(D and E)** Quantification of (D) apoptosis and (E) DNA synthesis in the indicated serum-starved cells after activation of c-Myc by addition of β -estradiol.

REFERENCES AND NOTES

1. K. B. Marcu, S. A. Bossone, A. J. Patel, *Annu. Rev. Biochem.* **61**, 809 (1992); D. S. Askew, R. A. Ashmun, B. C. Simmons, J. L. Cleveland, *Oncogene* **6**, 1915 (1991); Y. Shi *et al.*, *Science* **257**, 212 (1992); G. I. Evan and T. D. Littlewood, *Curr. Opin. Gen. Dev.* **3**, 44 (1993); M. E. Perry and A. J. Levine, *ibid.*, p. 50; L. A. Donehower and A. Bradley, *Biochim. Biophys. Acta* **1155**, 181 (1993).
2. G. I. Evan *et al.*, *Cell* **69**, 119 (1992).
3. C. Bello-Fernandez, G. Packham, J. L. Cleveland, *Proc. Natl. Acad. Sci. U.S.A.* **90**, 7804 (1993); N. Benvenisty, A. Leder, A. Kuo, P. Leder, *Genes Dev.* **6**, 2513 (1992); W. S. El-Deiry *et al.*, *Cell* **75**, 817 (1993).
4. M. Eilers, S. Schirm, J. M. Bishop, *EMBO J.* **10**, 133 (1991).
5. NIH 3T3-L1 fibroblasts or MEFs were transfected with plasmid DNA of the vector HH275.3 by the calcium phosphate method (17). This vector contains a bacterial gene for hygromycin B resistance and the human c-myc gene fused to sequences encoding the hormone binding domain of the human estrogen receptor (74). The fusion gene was expressed from a cytomegalovirus enhancer-promoter and tagged with the viral hemagglutinin 12CA5 epitope. Stable transfectants were selected in the presence of hygromycin B (200 μ g/ml). Cell culture was performed in pherol red-free medium. Single-cell clones were isolated and assayed for expression of c-MycER (6). Cells of a representative cell line (LM-3) were seeded on gridded cover slips and starved of serum for 48 hours in medium containing 0.5% fetal calf serum (FCS). The c-MycER was activated by addition of either β -estradiol (Merck, Darmstadt, Germany) or hydroxy-tamoxifen to the medium for 24 hours at a final concentration of 100 nM or 50 nM, respectively. BrdU (Amersham, Braunschweig, Germany) was added, and 6 hours later the cells were fixed in acetone-methanol (1:1) at -20°C for 10 min and blocked in 50% FCS for 15 min. Cells

- were incubated with antibody PAb 122 (15) for 45 min at room temperature, washed in phosphate-buffered saline, incubated with a Cy3-coupled goat antibody to mouse immunoglobulin G (Dianova, Hamburg, Germany) for 30 min, washed, and photographed. Cells were then denatured by 2 N HCl for 15 min at room temperature, washed, and incubated with a fluorescein-coupled mouse antibody to BrdU (Boehringer). Finally, cells were incubated 5 min with bisbenzamide H 33258 (1 μ g/ml) (Calbiochem, San Diego, CA) for chromatin staining. We determined the number of cells eliminated by apoptosis by counting cells within individual fields on the cover slip before, and 24 hours after, addition of β -estradiol. The determination was done with at least 2000 cells in four independent experiments for each cell line. The rate of DNA synthesis was evaluated as the ratio of BrdU-incorporating cells to viable cells 24 hours after addition of β -estradiol.
6. H. Hermeking and D. Eick, unpublished data.
 7. Serum-starved LM-3 cells were lysed in Laemmli buffer at various time points after addition of β -estradiol. Identical amounts of proteins were separated on a 12.5% polyacrylamide gel, transferred onto a nitrocellulose membrane, and probed with antibody PAb 240, which recognizes both mutant and denatured wt p53 protein (16) (Ab-3, Dianova). Signals were generated with the enhanced chemiluminescence detection system (Amersham) with a horseradish peroxidase-coupled secondary antibody (Promega, Heidelberg, Germany). Immunoblot analysis was performed as described (17).
 8. RNA was isolated, and identical amounts were separated on a 1% formaldehyde-agarose gel, transferred onto a nylon membrane (Hybond N+, Amersham), and hybridized with a 32 P-labeled murine p53 complementary DNA. The signals were measured with a PhosphorImager (Fuji). Northern (RNA) blot analysis was performed as described (17).
 9. N. C. Reich and A. J. Levine, *Nature* **308**, 199 (1984).
 10. M. B. Kastan, O. Onyekwere, D. Sidransky, B. Vogelstein, R. W. Craig, *Cancer Res.* **51**, 6304 (1991); M. B. Kastan *et al.*, *Cell* **71**, 587 (1992); X. Lu and D. P. Lane, *ibid.* **75**, 765 (1993).
 11. H. Hermeking *et al.*, *Proc. Natl. Acad. Sci. U.S.A.*, in press.
 12. L. A. Donehower *et al.*, *Nature* **356**, 215 (1992); M. Harvey *et al.*, *Oncogene* **8**, 2457 (1993).
 13. S. W. Lowe, H. E. Ruley, T. Jacks, D. E. Housman, *Cell* **74**, 957 (1993); S. W. Lowe and H. E. Ruley, *Genes Dev.* **7**, 535 (1993); M. Debbas and E. White, *ibid.*, p. 546.
 14. V. Kumar, S. Green, A. Staub, P. Chambon, *EMBO J.* **5**, 2231 (1986).
 15. E. G. Gurney, R. O. Harrison, J. Fenno, *J. Virol.* **34**, 752 (1980).
 16. J. V. Gannon, R. Greaves, R. Iggo, D. P. Lane, *EMBO J.* **9**, 1595 (1990).
 17. J. Sambrook, E. F. Fritsch, T. Maniatis, *Molecular Cloning: A Laboratory Manual* (Cold Spring Harbor Laboratory Press, Cold Spring Harbor, NY, ed. 2, 1989).
 18. We thank L. A. Donehower for p53^{-/-} cells; M. Eilers for NIH 3T3.LTR-MycER cells; P. Chambon for ER-cDNA (HE-14); G. Brander for PAb 122; G. Greene for ER-specific antibody H222; B. Kempkes for expression plasmids and technical advice; C. Dalke for oligonucleotides used for sequence analysis; A. Pullner for perfect technical assistance; and members of our institute for discussion and critical reading of the manuscript. Supported by the Deutsche Forschungsgemeinschaft (SFB190; Mechanismen und Faktoren der Genaktivierung) and Fonds der Chemischen Industrie.

26 May 1994; accepted 26 August 1994

Premature Microtubule-Dependent Cytoplasmic Streaming in *cappuccino* and *spire* Mutant Oocytes

William E. Theurkauf

Embryonic axis specification in *Drosophila melanogaster* is achieved through the asymmetric subcellular localization of morphogenetic molecules within the oocyte. The *cappuccino* and *spire* loci are required for both posterior and dorsoventral patterning. Time-lapse confocal microscopic analyses of living egg chambers demonstrated that these mutations induce microtubule reorganization and the premature initiation of microtubule-dependent ooplasmic streaming. As a result, microtubule organization is altered and bulk ooplasm rapidly streams during the developmental stages in which morphogens are normally localized. These changes in oocyte cytoarchitecture and dynamics appear to disrupt axial patterning of the embryo.

The functional asymmetries that specify the axes of the *Drosophila* embryo are established during oogenesis stages 8 through 10 (1–4). During these stages, the oocyte nucleus moves to the dorsal surface (5); *bicoid* mRNA, the primary anterior morphogen, is localized to the anterior cortex (6); *oskar* mRNA and the proteins encoded by *staußen* and *vasa*, which are required for posterior patterning and pole cell formation, are positioned at the posterior pole (3, 4, 7–9);

and *gurken* mRNA, which plays an essential role in dorsoventral axis specification, accumulates between the dorsally located oocyte nucleus and the cortex (10).

The microtubule cytoskeleton appears to play a key role in the establishment of axial asymmetry in *Drosophila* oocytes. Microtubule assembly inhibitors disrupt dorsal localization of the oocyte nucleus, anterior positioning of *bicoid* mRNA, and posterior accumulation of *oskar* mRNA and the protein encoded by *staußen* (11–13). Reorganization of the oocyte microtubule cytoskeleton is also temporally and morphologically

correlated with the initiation of morphogen localization (14). During stages 8 through 10, microtubules associate preferentially with the anterior cortex of the oocyte, so that a broad anterior to posterior cortical gradient is present at stage 9. This distribution of cortical microtubules mirrors the initial transient anterior localization of *oskar* mRNA and the anterior distribution of *bicoid* mRNA (14). The microtubule cytoskeleton reorganizes a second time during stage 10b, when the transfer of nurse cell cytoplasm and ooplasmic streaming begins (15). At this time, the anteroposterior microtubule network is replaced by arrays of parallel microtubules that form adjacent to the oocyte cortex (14). Inhibitor studies indicate that ooplasmic streaming is microtubule-dependent and is likely to be driven by organelle transport along the subcortical microtubules (14, 15).

Mutations at the *cappuccino* (*capu*) and *spire* (*spir*) loci alter both posterior and dorsoventral patterning, which raises the possibility that they affect the cytoskeletal functions that mediate axis specification (16). To determine if the *capu* and *spir* mutations influence axial polarization of the microtubule cytoskeleton, I injected living oocytes with rhodamine-conjugated tubulin and directly examined microtubules with laser scanning confocal microscopy (Fig. 1). Analysis of wild-type oocytes with this in vivo technique generally confirms the results of previous immunocytochemical studies (14). Oocytes from stages 8 through 10a contained a random network of cytoplasmic microtubules, with the highest density of microtubules associated with the anterior cortex (Fig. 1A). After initiation of ooplasmic streaming, during stage 10b, parallel arrays of microtubules could be observed just beneath the oocyte cortex (Fig. 1B). These subcortical microtubules persist through stage 12 and disassemble during stage 13, when streaming stops (17). The network of ooplasmic microtubules observed deep within living stage 8 through 10a oocytes was more extensive than that observed in fixed material. This difference may be the result of incomplete penetration of tubulin antibodies into the interior of the oocyte during immunolabeling (14).

The *capu* and *spir* mutations are identical in their effects on posterior and dorsoventral axis specification, which suggests that they define components of a single biochemical system (16). These mutations also produce similar changes in the organization of microtubules within the developing oocyte. Immunofluorescence analyses indicate that the *capu* and *spir* mutations do not affect microtubule organization during stages 2 through 6 (17). However, these mutations induce a change in the microtubule cytoskeleton during stages 8 through 10a. Early in stage 8, prominent sub-

Department of Biochemistry and Cell Biology, State University of New York, Stony Brook, NY 11794, USA.